Adaptive enumeration of implicit surfaces with affine arithmetic

Luiz Henrique de Figueiredo *Jorge Stolfi*

Relatório Técnico DCC–95-02

Março de 1995

Adaptive enumeration of implicit surfaces with affine arithmetic*

Luiz Henrique de Figueiredo† Jorge Stolfi‡

Abstract

We discuss adaptive enumeration and rendering methods for implicit surfaces, using octrees computed with affine arithmetic, a new tool for range analysis. Affine arithmetic is similar to standard interval arithmetic, but takes into account correlations between operands and sub-formulas, generally providing much tighter bounds for the computed quantities. The resulting octrees are accordingly much smaller, and the rendering faster. We also describe applications of affine arithmetic to intersection and ray tracing of implicit surfaces.

KEYWORDS: cellular models, interval analysis, rendering, implicit surfaces.

1 Introduction

Implicit surfaces have recently become popular in computer graphics and solid modeling. In order to exploit existing hardware and algorithms, it is often necessary to approximate such surfaces by models with simpler geometry, such as polygonal meshes or voxel arrays. Therefore, it is important to find efficient approximation methods for implicit surfaces.

Let S be a surface defined implicitly by the equation $h(x, y, z) = 0$. A simple and general technique for computing an approximation of S in a region Ω is:

1. decompose Ω into small cells;
2. identify which cells intersect S;
3. approximate S within each intersecting cell.

The enumeration of the intersecting cells is usually the most expensive step in this method. In the simplest schema, the cells that intersect S are identified by sampling. The function h is evaluated at the vertices of each cell; if the signs of those values are not identical, then the cell necessarily intersects S. Obviously, the converse does not hold: if

*An early version of this paper was presented at Implicit Surfaces '95.

†TeCGraf – Computer Graphics Technology Group, Computer Science Department, PUC–Rio, Rua Marquês de São Vicente 225, 22453–900 Rio de Janeiro, RJ, Brasil, lhf@icad.puc-rio.br

‡Computer Science Department (DCC/IMECC), Universidade Estadual de Campinas (UNICAMP), Caixa Postal 6065, 13081–970 Campinas, SP, Brasil, stolfi@dcc.unicamp.br

the values have all the same sign, we cannot conclude that the cell does not intersect S. This is a form of aliasing in the sampling related to the size of the cell. Therefore, cell sizes must be carefully chosen to avoid missing features due to undersampling.

Typically, the cellular decomposition of Ω is a regular grid of cubes. If there are n cubes along each main direction, then there are n^3 cubes to be scanned in a full enumeration, but only $O(n^2)$ cubes will intersect S. Thus, choosing a smaller cell size to avoid aliasing will greatly increase the number of cells to be scanned, and also increase the fraction of "useless" tests. Therefore, this approximation method is simple but not efficient.

Figure 1 shows a full enumeration of the curve defined implicitly by $y^2 - x^3 + x = 0$, in the square $\Omega = [-2 \,..\, 2] \times [-2 \,..\, 2]$, using a 16×16 grid. Intersecting cells were identified by sampling and appear in grey (note how few they are: only 44 out of 256). Black dots mark the points where the curve crosses cell edges; they can be joined to form a polygonal approximation to the curve.

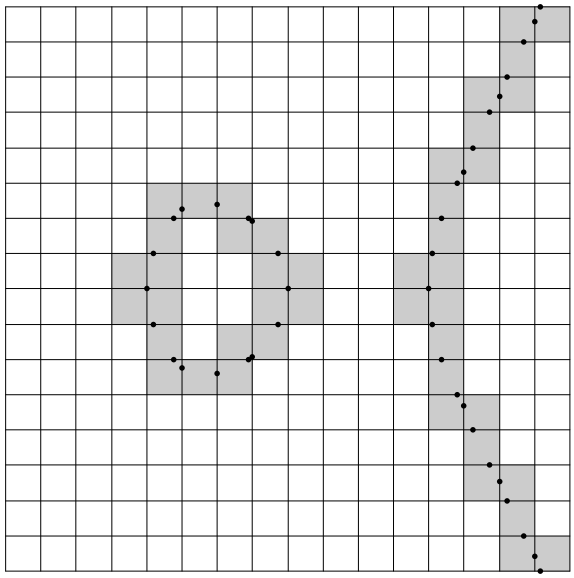

Figure 1: full enumeration of the curve given implicitly by $y^2 - x^3 + x = 0$

In Section 2, we review some general methods that try to find the cells that intersect S without enumerating all cells in Ω. The most reliable of those seems to be recursive subdivision of space based on *range analysis*, i.e., on estimates for the range of values taken by h on subsets of Ω. Interval arithmetic is the natural technique for range analysis. However, as we point out in Section 3, the excessive conservatism of interval arithmetic may greatly reduce the efficiency of the search. In Section 4, we describe *affine arithmetic*, a computation technique that generally provides much tighter bounds than interval arithmetic. In Section 5, we describe some experiments that exploit the properties of affine arithmetic to efficiently enumerate implicit surfaces. In Section 6, we show how to render implicit surfaces directly, during enumeration, without explicitly creating a cellular model. In Section 7, we discuss other applications of affine arithmetic for computing implicit objects. Finally, Section 8 contains some conclusions and outlines directions for future work.

2 Efficient enumeration methods

Several methods exist for finding the cells intersecting a surface S without visiting all cells in a cellular decomposition of a region Ω. The goal is to avoid testing all $O(n^3)$ cells, since only $O(n^2)$ cells intersect S.

The most popular efficient enumeration methods are still based on sampling. However, hierarchical decomposition methods are more efficient, more robust, and also suitable for parallel implementation. In this section, we review some of these methods.

2.1 Sampling-based methods

Continuation methods sample the surface only in the immediate neighbourhood of known intersecting cells [3, 4, 1, 6]. These methods only work for cellular subdivisions of Ω whose topology and geometry are well understood [6], so that it is simple to advance from one intersecting cell to an adjacent one, using "pivoting" techniques [1].

Adaptive refinement techniques start with a coarse cellular subdivision, and further subdivide only those cells that do intersect S [3, 10, 21]. Such techniques frequently use estimates of the curvature of S in a cell as an additional subdivision criterion, thus building a cellular subdivision that is adapted not only to the position of S inside Ω, but also to the intrinsic geometry of S. Polygonal approximations based on such subdivisions are thus quite efficient.

All these methods based on sampling have one fundamental difficulty, besides aliasing: finding a set of initial "seed" cells intersecting each connected component of S in Ω. (Unlike parametric surfaces, implicit surfaces can have several connected components; see Figure 1.) Obviously, if S is a general implicit surface, and we are restricted to evaluating h at individual points, then this problem has no satisfactory solution. Even if we assume that S has no extended features thinner than the minimum cell size (so that there are no aliasing problems), we still must sample the whole region Ω uniformly at that resolution; otherwise, we may miss some component of S.

2.2 Hierarchical decomposition methods

In order to discard large portions of Ω quickly and reliably, we need a more powerful test than point sampling. The latter can only prove the *presence* of S in some region of Ω; to reduce the number of cells scanned, we need a test procedure that can also prove the *absence* of S in a region.

The *hierarchical decomposition methods* rely on such a test to explore Ω recursively, starting with Ω itself as the initial cell. If a cell is proved to be empty, it is ignored; otherwise, it is subdivided into smaller cells, which are then explored recursively, until the cells are small enough to approximate S [18, 19, 7, 17, 20].

The meaning of "small enough" depends on the application. For rendering, it might mean "smaller than a pixel". For other applications, such as modeling, it may depend on some other numerical criterion. For instance, testing how closely the surface can be approximated by a linear function inside the cell allows polygonal approximations to adapt to the curvature of the surface.

Note that the test procedure is not required to be complete, in the sense that it may fail to prove either the presence or the absence of S in a given cell. In particular, a cell that is declared "small enough" may still have unknown status. Each application must decide what to do with those "indeterminate" cells: discard them, treat them just like the cells that do intersect S, or handle them in some special way. Point sampling may be useful at this stage to help identify some intersecting cells.

The subdivision of Ω resulting from a hierarchical decomposition is not a regular grid, but rather a tree of nested cells. The leaves in this tree form a cellular model for S. There are many variants of this method; they differ in the shape of cells and the method of subdivision. In particular, if the cells are cubical and divided into eight equal parts, then the resulting subdivision is called an *octree* [16]. Other choices give *binary space partitions* [8], 3-*d trees* [2], *hierarchical triangulations* [15], and many more.

3 Interval arithmetic

In order to prove that a given cell C does not intersect S, we must prove that the function h does not vanish inside C. For some classes of surfaces, this fact can usually be established by specific tests. For instance, if h is a polynomial, we can compute its Bézier-Bernstein coefficients for that cell: if they are all positive, or all negative, then the same will be true of h. Unfortunately, this method cannot be used for general (non-polynomial) functions; or even for polynomials of high degree presented in factored form, such as $(x^2 + y^2 + z^4)^{20} - 1$.

Range analysis can be used to provide general test procedures for hierarchical decompositions. In range analysis, an estimate is computed for the whole range of values taken by the function h on the points of a cell C. This estimate is an interval *guaranteed* to contain $h(C)$. If this interval does not contain zero, then the function h cannot vanish inside C and the test has proved that the cell does not intersect S. However, if the interval does contains zero, we cannot conclude that the cell intersects S because estimates are not required to be exact.

The classical technique of *interval arithmetic* (IA), also known as *interval analysis*, provides a natural tool for range analysis. In IA, each quantity is represented by an interval of floating-point numbers. Those intervals are added, subtracted, multiplied, etc., in such a way that each computed interval is guaranteed to contain the (unknown) value of the quantity it represents [14].

To test whether a cell C intersects the surface S, we can evaluate $h(x, y, z)$ with IA, letting x, y and z be the projections of the cell onto the coordinate axes. The interval thus computed will contain all values of h for points inside the cell. If this interval is entirely positive, or entirely negative, then we have proved that C does not intersect S.

Hierarchical decomposition methods based on IA have recently been proposed for the enumeration of implicit surfaces in computer graphics applications [19, 7, 17]. Those methods have become quite popular, due to their ability to handle arbitrarily complex non-polynomial surfaces, and their immunity to round-off errors.

Figure 2 shows a hierarchical enumeration based on IA of the curve shown in Figure 1, but now using a 32×32 grid. Note that large portions of Ω were discarded at early stages.

Section 5 contains other examples.

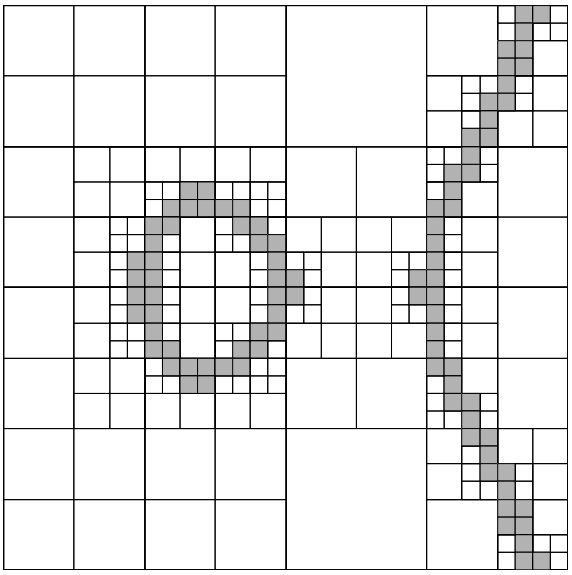

Figure 2: hierarchical enumeration of $y^2 - x^3 + x = 0$

3.1 The error explosion problem

The main weakness of IA is that it tends to be too conservative: the computed interval for a quantity may be much wider than the true range of that quantity, often to the point of uselessness. This over-conservatism is mainly due to the assumption that the (unknown) values of the arguments to primitive operations may vary *independently* over the given interval If there are any mathematical constraints between these arguments, then not all combinations of values in the corresponding intervals will be valid. In that case, the result interval computed by IA may be much wider than the true range of the result quantity.

For example, consider evaluating $x(10 - x)$, where x is known to lie in the interval $\bar{x} = [4 .. 6]$. Applying the IA formulas blindly, we get

$$\begin{aligned} 10 - \bar{x} &= [10 .. 10] - [4 .. 6] = [4 .. 6] \\ \bar{x}(10 - \bar{x}) &= [4 .. 6] \cdot [4 .. 6] = [16 .. 36], \end{aligned}$$

which is 20 times wider than the true range of the expression $x(10 - x)$ over $[4 .. 6]$, namely $[24 .. 25]$. The large discrepancy between the two intervals is due to the inverse relation between the quantities x and $10 - x$, which is not known to the IA multiplication algorithm.

The over-conservatism of IA is particularly bad in long computation chains, where the intervals computed by one stage of the chain are the inputs to the following stage. In such cases, one often observes an "error explosion": as the evaluation advances down the chain, the relative accuracy of the computed intervals decreases exponentially, and they soon become too wide to be useful, by many orders of magnitude. Unfortunately, long computations chains are not uncommon in computer graphics applications.

4 Affine arithmetic

To address the "error explosion" problem in IA, Comba and Stolfi [5] proposed a new model for numerical computation, called *affine arithmetic* (AA). Like standard IA, affine arithmetic keeps track automatically of the round-off and truncation errors affecting each computed quantity. Unlike IA, however, affine arithmetic keeps track of *correlations* between those quantities. Thanks to this extra information, AA is able to provide much tighter intervals than IA, especially in long computation chains.

The key feature of AA is an extended encoding of quantities from which one can determine, in addition to their ranges, also certain relationships to other quantities — such as the ones existing between x and $10 - x$ in the example. Specifically, a partially unknown quantity x is represented in AA by an *affine form* $\hat{x}$, which is a first-degree polynomial:

$$\hat{x} = x_0 + x_1\varepsilon_1 + x_2\varepsilon_2 + \cdots + x_n\varepsilon_n.$$

Here, the x_i are known real coefficients (stored as floating-point numbers), and the ε_i are symbolic variables whose values are unknown but assumed to lie in the interval $\mathbf{U} = [-1 .. +1]$.

Each ε_i is called a *noise symbol*: it stands for an independent source of error or uncertainty that contributes to the total uncertainty of the quantity x; the corresponding coefficient x_i gives the magnitude of that contribution. The source of error may be external (due to original uncertainty in some input quantity) or internal (due to round-off and truncation errors committed in the computation of $\hat{x}$).

A somewhat similar approach has been proposed by Hansen [11], in which quantities are represented instead by affine combinations of a *fixed* number of *intervals*. In AA, new noise symbols are dynamically created during a long computation (Section 4.3).

As one may expect, affine arithmetic is more complex and expensive than ordinary interval arithmetic. However, its higher accuracy is worth the extra cost in many applications, including adaptive enumeration of implicit objects, as we show in Section 5.

4.1 Conversions between IA and AA

If $\hat{x} = x_0 + x_1\varepsilon_1 + \cdots + x_n\varepsilon_n$ is an affine form for a quantity x, then the value of x is guaranteed to be in the *range* of $\hat{x}$, which is the interval

$$[\hat{x}] = [x_0 - \xi .. x_0 + \xi], \quad \xi = \sum_{i=1}^{n} |x_i| .$$

Note that $[\hat{x}]$ is the smallest interval that contains all possible values of $\hat{x}$, assuming that each ε_i ranges independently over the interval $\mathbf{U} = [-1 .. +1]$.

Conversely, given an interval $\bar{x} = [a .. b]$ representing some quantity x in IA, an equivalent affine form for the same quantity is given by $\hat{x} = x_0 + x_k\varepsilon_k$, where

$$x_0 = \frac{b+a}{2} \quad \text{and} \quad x_k = \frac{b-a}{2} .$$

The noise symbol ε_k symbolizes the uncertainty in the value of x. Since the interval $\bar{x}$ tells us nothing about possible constraints between the value of x and that of other variables, ε_k must be distinct from all other noise symbols previously used in the same computation.

4.2 Exploiting correlations in operands

The key feature of AA is that the same noise symbol ε_i may contribute to the uncertainty of two or more quantities (inputs, outputs, or intermediate results) arising in the evaluation of an expression. The sharing of a noise symbol ε_i by two affine forms $\hat{x}$, $\hat{y}$ indicates some partial dependency between the underlying quantities x, y. The magnitude and sign of the dependency is determined by the corresponding coefficients x_i, y_i.

For example, suppose that the quantities x, y are represented by the affine forms

$$\begin{aligned} \hat{x} &= 10 + 2\varepsilon_1 + 1\varepsilon_2 \qquad - 1\varepsilon_4 \\ \hat{y} &= 20 - 3\varepsilon_1 \qquad + 1\varepsilon_3 + 4\varepsilon_4. \end{aligned}$$

From this data, we can tell that x lies in the interval $[6 \,..\, 14]$ and y lies in $[12 \,..\, 28]$. However, since they both include the same noise variables ε_1 and ε_4 with non-zero coefficients, they are not entirely independent of each other. In fact, the pair (x, y) is constrained to lie in the region of $\mathbf{R}^2$ depicted in Figure 3 (dark grey), which is substantially smaller than the rectangle $[6 \,..\, 14] \times [12 \,..\, 28]$ (light grey). Obviously, this dependency information would be lost if we were to replace $\hat{x}$ and $\hat{y}$ by the ordinary intervals $[\hat{x}]$ and $[\hat{y}]$, even though the latter encode precisely the same ranges of values as the former.

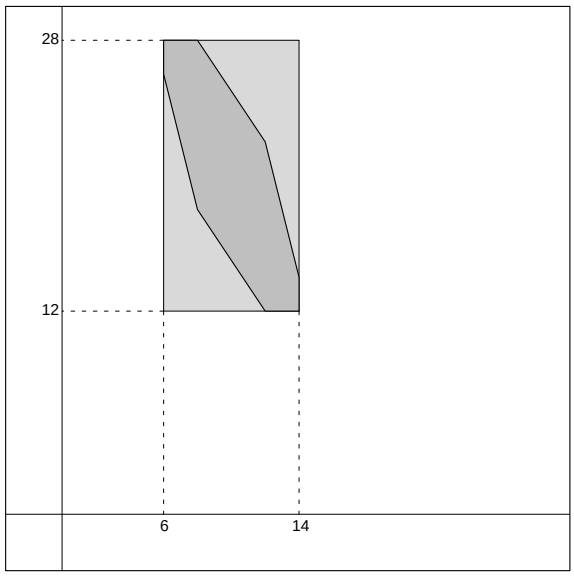

Figure 3: joint range of two quantities x and y, where $\hat{x} = 10 + 2\varepsilon_1 + 1\varepsilon_2 - 1\varepsilon_4$ and $\hat{y} = 20 - 3\varepsilon_1 + 1\varepsilon_3 + 4\varepsilon_4$

4.3 Computing with affine arithmetic

To evaluate a formula in AA, we must replace each of its elementary operations $z \leftarrow f(x,y)$ on real numbers by an equivalent operation $\hat{z} \leftarrow \hat{f}(\hat{x},\hat{y})$ on affine forms, where $\hat{f}$ is a procedure that computes an affine form for $z = f(x,y)$ that is consistent with $\hat{x},\hat{y}$.

When f is an affine function of x,y, the value $\hat{z}$ can be expressed exactly as an affine combination of the noise symbols ε_i. More precisely, if

$$\begin{aligned} \hat{x} &= x_0 + x_1\varepsilon_1 + \cdots + x_n\varepsilon_n \\ \hat{y} &= y_0 + y_1\varepsilon_1 + \cdots + y_n\varepsilon_n, \end{aligned}$$

and $\alpha \in \mathbf{R}$, then

$$\begin{aligned} \hat{x} \pm \hat{y} &= (x_0 \pm y_0) + (x_1 \pm y_1)\varepsilon_1 + \cdots + (x_n \pm y_n)\varepsilon_n \\ \alpha\hat{x} &= (\alpha x_0) + (\alpha x_1)\varepsilon_1 + \cdots + (\alpha x_n)\varepsilon_n \\ \hat{x} \pm \alpha &= (x_0 \pm \alpha) + x_1\varepsilon_1 + \cdots + x_n\varepsilon_n. \end{aligned}$$

Note that, according to those formulas, the difference $\hat{x} - \hat{x}$ between an affine form and itself is identically zero. In this case, the fact that the two operands share the same noise symbols with the same coefficients reveals that they are actually the same quantity, and not just two quantities that happen to have the same range of possible values. Thanks to this feature, in AA we also have $(\hat{x} + \hat{y}) - \hat{x} = \hat{y}$, $(3\hat{x}) - \hat{x} = 2\hat{x}$, and so on. Such properties are *not* valid in IA, and are one source of error explosion.

When f is not an affine operation, $\hat{z}$ cannot be expressed exactly as an affine combination of the ε_i. In that case, we pick the best affine approximation (best in the Chebyshev sense of minimizing the maximum error), and then append an extra term $z_k\varepsilon_k$ to represent the error introduced by this approximation:

$$\hat{z} = z_0 + z_1\varepsilon_1 + \cdots + z_n\varepsilon_n + z_k\varepsilon_k.$$

Here, ε_k must be a brand new noise symbol (distinct from all other noise symbols in the same computation) and z_k must be an upper bound for the approximation error. Note that, unlike Hansen's generalized interval arithmetic, new noise symbols are created during a long AA computation.

Using this approach, the multiplication of two affine forms $\hat{x}$, $\hat{y}$ is given by

$$\begin{aligned} z_0 &= x_0 y_0 \\ z_i &= x_0 y_i + y_0 x_i \qquad (i = 1, \ldots, n) \\ z_k &= uv, \end{aligned}$$

where

$$u = \sum_{i=1}^{n} |x_i|\,, \qquad v = \sum_{i=1}^{n} |y_i|\,.$$

Similar formulas can be given for the other elementary operations and functions. For instance, it turns out [5] that the square root of an affine form $\hat{x} = x_0 + x_1\varepsilon_1 + \cdots + x_n\varepsilon_n$

is given by

$$\begin{aligned} z_0 &= \alpha x_0 + \beta \\ z_i &= \alpha x_i \qquad\qquad (i = 1, \ldots, n) \\ z_k &= \delta, \end{aligned}$$

where

$$\begin{aligned} \alpha &= \frac{1}{\sqrt{a} + \sqrt{b}} \\ \beta &= \frac{\sqrt{a} + \sqrt{b}}{8} + \frac{1}{2}\frac{\sqrt{a}\sqrt{b}}{\sqrt{a} + \sqrt{b}} \\ \delta &= \frac{1}{8}\frac{(\sqrt{b} - \sqrt{a})^2}{\sqrt{a} + \sqrt{b}} \end{aligned}$$

and $[a \,..\, b]$ is the interval $[\hat{x}]$.

4.4 Example revisited

Consider again evaluating $z = x(10 - x)$, for x in the interval $[4 \,..\, 6]$, but now using AA instead of IA:

$$\begin{aligned} \hat{x} &= 5 + 1\varepsilon_1 \\ 10 - \hat{x} &= 5 - 1\varepsilon_1 \\ \hat{z} = \hat{x}(10 - \hat{x}) &= 25 + 0\varepsilon_1 - 1\varepsilon_2. \end{aligned}$$

Observe that the influence of the noise symbol ε_1 in the factors happened to cancel out (to first order) in the product.

The range of z implied by the affine form $\hat{z}$ is

$$[\hat{z}] = [25 - 1 \,..\, 25 + 1] = [24 \,..\, 26],$$

which is much closer to $[24 \,..\, 25]$, the true range of z. Recall that IA gave $[16 \,..\, 36]$ for this expression.

5 Examples of adaptive enumeration

In this section, we show examples that compare the performance of IA and AA in adaptive enumeration. Because pictures of three dimensional decompositions are not easy to understand, we only give pictures of the enumeration of two-dimensional implicit curves.

In all these examples, the goal is to build a cellular model of a curve given implicitly by $h(x, y) = 0$ inside some rectangle Ω. The model consists of a set of cells from some fixed regular grid, whose union is guaranteed to contain all zeros of h in Ω. These cells are shown in grey in the pictures.

5.1 A quartic

Take the quartic curve defined by

$$h(x,y) = x^2 + y^2 + xy - (xy)^2/2 - 1/4$$

in the square $\Omega = [-2\ ..\ 2] \times [-2\ ..\ 2]$, using a 32×32 grid of cells. In a full enumeration, $1024 = 32 \cdot 32$ cells have to be scanned, but the curve actually enters only 66 of these cells.

Figure 4 illustrates an adaptive enumeration with interval arithmetic and affine arithmetic, using a 2-d tree. With IA, the range of h was evaluated 847 times and 246 cells remained in the model (i.e., could not be shown to be disjoint from the curve). With AA, the range of h was evaluated 451 times and only 70 cells remained in the model. Thus, IA generated a model with 180 useless cells whereas AA generated a model with only 4 useless cells, even at such a relatively low resolution.

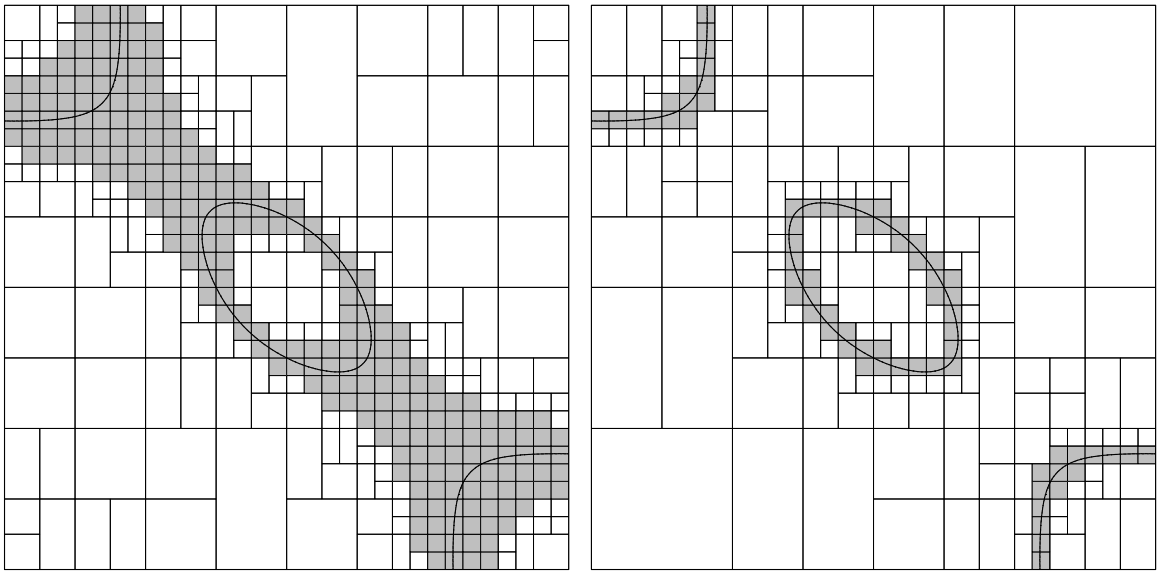

Figure 4: adaptive enumeration of quartic with IA (left) and AA (right)

5.2 Quadratic electrostatic potential

Consider now the "quadratic" electrostatic potential defined by n charges q_i located at points (x_i, y_i):

$$h(x,y) = \sum_{i=1}^{n} \frac{q_i}{(x - x_i)^2 + (y - y_i)^2} \ .$$

(True electrostatic potential depends on distances, not on square of distances.) In this case, the interesting curves are the equipotential curves $h(x,y) = h_0$. Such "potential" functions and their variations are useful for modeling with implicit objects [22].

Figure 5 illustrates an adaptive quadtree enumeration with interval arithmetic and affine arithmetic of an equipotential curve for the quadratic electrostatic potential defined by four

equal charges. The grid is 64×64; a full enumeration would have to scan 4096 cells. In both cases, the range of h was evaluated 1449 times (a coincidence). However, 346 cells remained in the model generated by IA, whereas only 299 remained in the model generated by AA.

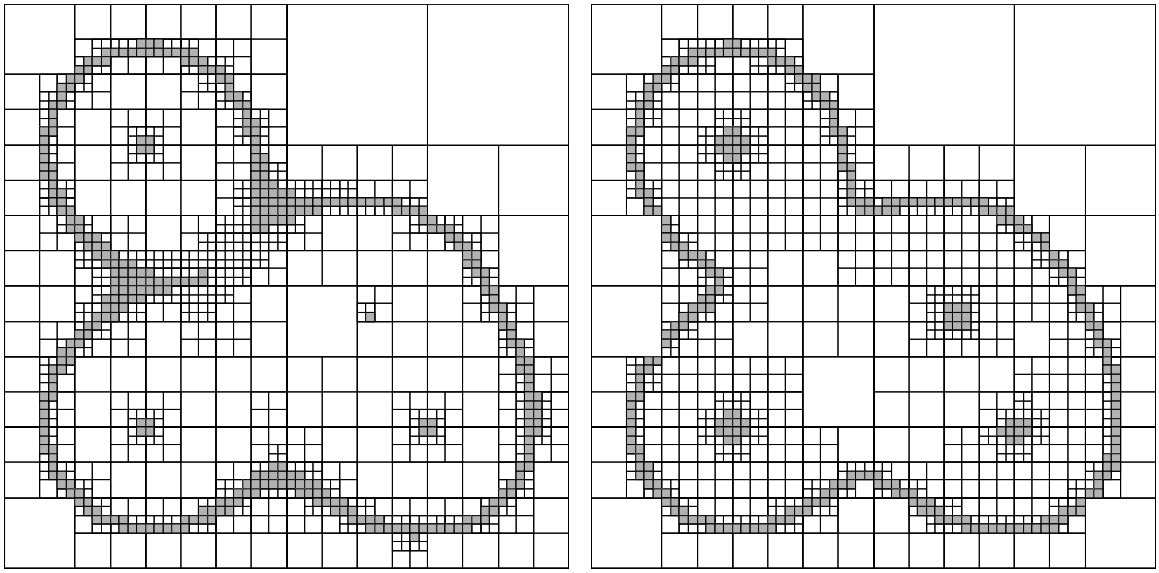

Figure 5: adaptive enumeration of quadratic electrostatic potential with IA (left) and AA (right)

5.3 The quartic in 3d

As a three-dimensional example, consider an octree enumeration of the quartic surface defined by

$$h(x, y, z) = x^2 + y^2 + xy - (xy)^2/2 - 1/4 - z,$$

in the cube $\Omega = [-2 \,..\, 2] \times [-2 \,..\, 2] \times [-2 \,..\, 2]$.

We give two tables showing how the size of the model (number of leaves in the octree) and the time (in seconds) taken to compute it depend on the resolution of the underlying grid (the resolution is $n = 2^L$ at level L). Table 1 shows this data for IA; Table 2 shows this data for AA. Times were measured in an otherwise idle SPARCstation 10.

We observe that AA evaluates h half as many times as IA, and generates a model half the size of the model generated by IA: the size of the IA model is approximately $5n^2$, whereas the size of the AA model is approximately $2.4n^2$. However, AA is 4.3 times slower than IA: the time for the IA model is approximately $86n^2\mu$sec whereas the time for the AA model is approximately $370n^2\mu$sec (note that the time is linear in the size of the model.)

level	evaluations	leaves	time
1	9	8	0.0
2	73	62	0.0
3	569	334	0.0
4	3241	1276	0.1
5	13449	5122	0.2
6	54425	20580	0.4
7	219065	82502	1.5
8	879081	329746	5.7
9	3517049	1318058	22.5
10	14061513	5275400	89.5

Table 1: performance of adaptive enumeration of 3d quartic with IA

level	evaluations	leaves	time
1	9	8	0.0
2	73	56	0.0
3	521	190	0.1
4	2041	710	0.2
5	7721	2664	0.5
6	29033	10104	1.7
7	109865	39960	6.4
8	429545	158282	24.8
9	1695801	630380	97.8
10	6738841	2516356	388.5

Table 2: performance of adaptive enumeration of 3d quartic with AA

6 Rendering

The octrees built during enumeration can be used to speed up ray tracing algorithms [9, 23]. However, a "lower" quality rendering can be done directly, concurrently with the enumeration; there is no need to explicitly build an octree.

By composing the function h with the appropriate projective map, we can take the domain Ω to be a rectangular box, aligned with the coordinate axes, and compute the image of the orthogonal projection of the surface S defined by h onto a horizontal plane located above the box Ω. For simplicity, we assume that the resolution of the image is $n \times n$, where $n = 2^L$. The enumeration proceeds down the octree to level L. When we reach a leaf of the octree (i.e., a cell at level L), we compute the colour of the corresponding pixel in the image. Each cell has an integer address (x, y, z); all cells with the same x, y project onto the same pixel (x, y). To remove hidden parts, we use a "painter's algorithm", carefully traversing the octree from bottom to top (in the z direction).

In order to compute the colour of a pixel in shaded images of S, we need to compute also the mean normal direction to S in the cell corresponding to the pixel. The normal direction is the direction of the gradient of h. Full enumeration and adaptive enumeration with interval arithmetic do not directly provide an estimate for ∇h. For full enumeration, one typically uses an estimate based on central differences [12]. For adaptive enumeration with interval arithmetic, techniques such as formal differentiation (evaluated in either floating point or IA) or Bauer–Strassen differentiation [13] would be required to estimate ∇h in each visible cell. On the other hand, affine arithmetic directly provides an estimate for ∇h. Recall that, to compute h in a cell represented by the intervals $\bar{x}$, $\bar{y}$, $\bar{z}$, we take the corresponding affine forms $\hat{x} = x_0 + x_1\varepsilon_1$, $\hat{y} = y_0 + y_2\varepsilon_2$, $\hat{z} = z_0 + z_3\varepsilon_3$, and compute $\hat{h} = h_0 + h_1\varepsilon_1 + h_2\varepsilon_2 + h_3\varepsilon_3 + \ldots$ Then we can take $(h_1/x_1, h_2/y_2, h_3/z_3)$ as an estimate for the mean value of ∇h in this cell, and from this estimate compute an appropriate colour for the corresponding pixel in the image.

Figure 6 shows a 256×256 image of the union of two spheres rendered using this technique.

7 Other applications

Affine arithmetic is also useful for other applications related to implicit objects. We describe two such applications briefly: surface intersection, and rendering with ray tracing.

7.1 Intersection of implicit surfaces

The intersection of two implicit surfaces defined by functions f and g can be given implicitly by a single function $h = f^2 + g^2$. This expression is not useful for enumeration based on point sampling because h is always positive and enumeration based on sampling relies on changes of sign in h to identify intersecting cells. On the other hand, enumeration using range analysis is perfectly feasible in this case. Again, affine arithmetic will be able to exploit the correlations present in the expression of h to compute tighter bounds. Alternatively, the

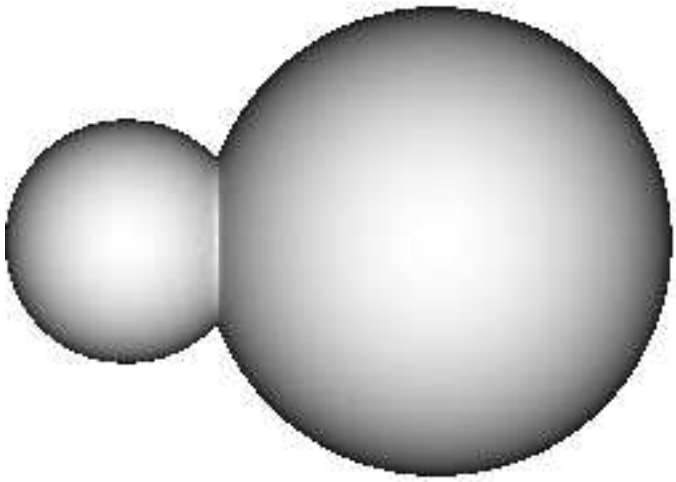

Figure 6: the union of two spheres enumerated and shaded with AA

enumeration for the intersection can be done by combining the simultaneous enumeration of the two surfaces, rejecting cells that are rejected in at least one enumeration.

7.2 Ray tracing

A fundamental step in ray tracing a surface is finding the first intersection of a ray with the surface. If the surface is given implicitly by $h(x, y, z) = 0$, and the ray is the line segment $\overrightarrow{pq}$, then one needs to find the smallest root of the univariate function

$$f(t) = h((1-t)x_p + tx_q,\ (1-t)y_p + ty_q,\ (1-t)z_p + tz_q),$$

in the interval $t \in [0\ ..\ 1]$.

A simple algorithm for finding all roots of f is the following. Evaluate $\bar{u} = \bar{f}(\bar{t})$ using IA, for the whole interval $\bar{t} = [0\ ..\ 1]$. If the resulting interval $\bar{u}$ is strictly positive or strictly negative, then the ray does not intersect the surface. Otherwise, split $\bar{t}$ in two equal parts, and recursively search each half. Stop the recursion when the interval $\bar{t}$ is small enough for the application. A simple variant of this algorithm finds the smallest root: only search the right half if the left half has been shown to contain no roots.

One drawback of this algorithm is that evaluating $\bar{f}(\bar{t})$ with IA is equivalent to evaluating $\bar{h}(\bar{x}, \bar{y}, \bar{z})$ on the intervals $\bar{x} = [x_p\ ..\ x_q]$, $\bar{y} = [y_p\ ..\ y_q]$, $\bar{z} = [z_p\ ..\ z_q]$ — that is, evaluating h on the axis-aligned bounding box of the segment pq, instead of only along the segment itself. Again, the problem arises because IA does not know that the arguments $\bar{x}$, $\bar{y}$, and $\bar{z}$ of $\bar{h}$ are highly correlated. Obviously, the bounding box of the segment pq may intersect the surface even when the segment itself does not.

Replacing standard IA by affine arithmetic will generally improve the performance of this algorithm. Even without any algebraic manipulation, AA will automatically notice that the affine forms $\hat{x}$, $\hat{y}$, and $\hat{z}$ are strongly correlated, and thus will usually produce tighter bounds for $f(\hat{t})$. Moreover, as we have seen above, AA also automatically provides

estimates for the derivative of f, allowing us to replace the binary search used in the IA method by Newton's method, without explicitly computing derivatives.

8 Conclusion

Numerical experiments show that affine arithmetic is indeed more accurate than standard interval arithmetic. On the other hand, AA is more complex and expensive than IA. However, its higher accuracy is worth the extra cost for adaptive enumeration of implicit objects because the models resulting from enumeration with AA are smaller. Although the relative speeds of IA and AA depend on the particular function being evaluated, in our implementation, AA is typically 4–5 times slower than IA. Work is in progress to improve the performance of AA.

An interesting extension of the techniques described here would be to use the extra information provided by AA to estimate surface curvature, so that the enumeration is adapted not only to the location of the surface in the ambient space, but also to its intrinsic geometry, as adaptive refinement techniques do.

Acknowledgements. We thank João Comba, who helped implement a prototype AA package in Modula-3, and Marcus Vinicius Andrade, who helped debug the C version and wrote an implicit surface ray-tracer based on it. This work was performed on equipment kindly ceded by Paulo Correa de Mello (Chemistry Dept., PUC-Rio), and on equipment acquired within a FAPESP thematic project. The authors are partially supported by research and development grants from the Brazilian Council for Scientific and Technological Development (CNPq). Some of this research was performed while the second author was at the DEC Systems Research Center (SRC) in Palo Alto.

References

[1] E. L. Allgower and K. Georg. *Numerical Continuation Methods: An Introduction.* Springer-Verlag, 1990.

[2] J. L. Bentley. Multidimensional binary search trees used for associative searching. *Communications of the ACM*, 18:509–517, 1975.

[3] J. Bloomenthal. Polygonization of implicit surfaces. *Computer Aided Geometric Design*, 5(4):341–355, November 1988.

[4] R. E. Chandler. A tracking algorithm for implicitly defined curves. *IEEE Computer Graphics and Applications*, 8(2):83–89, March 1988.

[5] J. L. D. Comba and J. Stolfi. Affine arithmetic and its applications to computer graphics. In *Proceedings of VI SIBGRAPI (Brazilian Symposium on Computer Graphics and Image Processing)*, pages 9–18, 1990.

[6] D. P. Dobkin, S. V. F. Levy, W. P. Thurston, and A. R. Wilks. Contour tracing by piecewise linear approximations. *ACM Transactions on Graphics*, 9(4):389–423, October 1990.

[7] T. Duff. Interval arithmetic and recursive subdivision for implicit functions and constructive solid geometry. *Computer Graphics (SIGGRAPH '92 Proceedings)*, 26(2):131–138, July 1992.

[8] H. Fuchs, Z. M. Kedem, and B. F. Naylor. On visible surface generation by a priori tree structures. *Computer Graphics (SIGGRAPH '80 Proceedings)*, 14(3):124–133, July 1980.

[9] A. S. Glassner. Space subdivision for fast ray tracing. *IEEE Computer Graphics and Applications*, 4(10):15–22, October 1984.

[10] M. Hall and J. Warren. Adaptive polygonalization of implicitly defined surfaces. *IEEE Computer Graphics and Applications*, 10(6):33–42, November 1990.

[11] E. R. Hansen. A generalized interval arithmetic. *Lecture Notes in Computer Science*, 29:7–18, 1975.

[12] M. Levoy. Display of surfaces from volume data. *IEEE Computer Graphics and Applications*, 8(3):29–37, May 1988.

[13] Yu. V. Matijasevich. A posteriori interval analysis. *Lecture Notes in Computer Science*, 204:328–334, 1985.

[14] R. E. Moore. *Interval Analysis*. Prentice-Hall, 1966.

[15] R. M. Persiano, M. Salim, and L. P. Bueno. Boundary evaluation of CSG solids by simplicial subdivision. In *COMPUGRAPHICS '91*, volume II, pages 220–229, 1991.

[16] H. Samet. *Applications of Spatial Data Structures*. Addison-Wesley, 1990.

[17] J. M. Snyder. Interval analysis for computer graphics. *Computer Graphics (SIGGRAPH '92 Proceedings)*, 26(2):121–130, July 1992.

[18] K. G. Suffern. Quadtree algorithms for contouring functions of two variables. *The Computer Journal*, 33:402–407, 1990.

[19] K. G. Suffern and E. D. Fackerell. Interval methods in computer graphics. *Computers & Graphics*, 15:331–340, 1991.

[20] G. Taubin. Rasterizing algebraic curves and surfaces. *IEEE Computer Graphics and Applications*, 14:14–23, 1994.

[21] L. Velho. Adaptive polygonization of implicit surfaces using simplicial decomposition and boundary constraints. In *Eurographics '90*, pages 125–136, 1990.

[22] B. Wyvill and G. Wyvill. Field functions for implicit surfaces. *The Visual Computer*, 5(1/2):75–82, March 1989.

[23] G. Wyvill, T. L. Kunii, and Y. Shirai. Space division for ray tracing in CSG. *IEEE Computer Graphics and Applications*, 6(4):28–34, April 1986.

Relatórios Técnicos – 1992

92-01 **Applications of Finite Automata Representing Large Vocabularies,** *C. L. Lucchesi, T. Kowaltowski*

92-02 **Point Set Pattern Matching in d-Dimensions,** *P. J. de Rezende, D. T. Lee*

92-03 **On the Irrelevance of Edge Orientations on the Acyclic Directed Two Disjoint Paths Problem,** *C. L. Lucchesi, M. C. M. T. Giglio*

92-04 **A Note on Primitives for the Manipulation of General Subdivisions and the Computation of Voronoi Diagrams,** *W. Jacometti*

92-05 **An (l, u)-Transversal Theorem for Bipartite Graphs,** *C. L. Lucchesi, D. H. Younger*

92-06 **Implementing Integrity Control in Active Databases,** *C. B. Medeiros, M. J. Andrade*

92-07 **New Experimental Results For Bipartite Matching,** *J. C. Setubal*

92-08 **Maintaining Integrity Constraints across Versions in a Database,** *C. B. Medeiros, G. Jomier, W. Cellary*

92-09 **On Clique-Complete Graphs,** *C. L. Lucchesi, C. P. Mello, J. L. Szwarcfiter*

92-10 **Examples of Informal but Rigorous Correctness Proofs for Tree Traversing Algorithms,** *T. Kowaltowski*

92-11 **Debugging Aids for Statechart-Based Systems,** *V. G. S. Elias, H. Liesenberg*

92-12 **Browsing and Querying in Object-Oriented Databases,** *J. L. de Oliveira, R. de O. Anido*

Relatórios Técnicos – 1993

93-01 **Transforming Statecharts into Reactive Systems,** *Antonio G. Figueiredo Filho, Hans K. E. Liesenberg*

93-02 **The Hierarchical Ring Protocol: An Efficient Scheme for Reading Replicated Data,** *Nabor das C. Mendonça, Ricardo de O. Anido*

93-03 **Matching Algorithms for Bipartite Graphs,** *Herbert A. Baier Saip, Cláudio L. Lucchesi*

93-04 **A lexBFS Algorithm for Proper Interval Graph Recognition,** *Celina M. H. de Figueiredo, João Meidanis, Célia P. de Mello*

93-05 **Sistema Gerenciador de Processamento Cooperativo,** *Ivonne. M. Carrazana, Nelson. C. Machado, Célio. C. Guimarães*

93-06 **Implementação de um Banco de Dados Relacional Dotado de uma Interface Cooperativa,** *Nascif A. Abousalh Neto, Ariadne M. B. R. Carvalho*

93-07 **Estadogramas no Desenvolvimento de Interfaces,** *Fábio N. de Lucena, Hans K. E. Liesenberg*

93-08 **Introspection and Projection in Reasoning about Other Agents,** *Jacques Wainer*

93-09 **Codificação de Seqüências de Imagens com Quantização Vetorial,** *Carlos Antonio Reinaldo Costa, Paulo Lício de Geus*

93-10 **Minimização do Consumo de Energia em um Sistema para Aquisição de Dados Controlado por Microcomputador,** *Paulo Cesar Centoducatte, Nelson Castro Machado*

93-11 **An Implementation Structure for RM-OSI/ISO Transaction Processing Application Contexts,** *Flávio Morais de Assis Silva, Edmundo Roberto Mauro Madeira*

93-12 **Boole's conditions of possible experience and reasoning under uncertainty,** *Pierre Hansen, Brigitte Jaumard, Marcus Poggi de Aragão*

93-13 **Modelling Geographic Information Systems using an Object Oriented Framework,** *Fatima Pires, Claudia Bauzer Medeiros, Ardemiris Barros Silva*

93-14 **Managing Time in Object-Oriented Databases,** *Lincoln M. Oliveira, Claudia Bauzer Medeiros*

93-15 **Using Extended Hierarchical Quorum Consensus to Control Replicated Data: from Traditional Voting to Logical Structures,** *Nabor das Chagas Mendonça, Ricardo de Oliveira Anido*

93-16 $\mathcal{LL}$ – **An Object Oriented Library Language Reference Manual,** *Tomasz Kowaltowski, Evandro Bacarin*

93-17 **Metodologias para Conversão de Esquemas em Sistemas de Bancos de Dados Heterogêneos,** *Ronaldo Lopes de Oliveira, Geovane Cayres Magalhães*

93-18 **Rule Application in GIS – a Case Study,** *Claudia Bauzer Medeiros, Geovane Cayres Magalhães*

93-19 **Modelamento, Simulação e Síntese com VHDL,** *Carlos Geraldo Krüger e Mário Lúcio Côrtes*

93-20 **Reflections on Using Statecharts to Capture Human-Computer Interface Behaviour,** *Fábio Nogueira de Lucena e Hans Liesenberg*

93-21 **Applications of Finite Automata in Debugging Natural Language Vocabularies,** *Tomasz Kowaltowski, Cláudio Leonardo Lucchesi e Jorge Stolfi*

93-22 **Minimization of Binary Automata,** *Tomasz Kowaltowski, Cláudio Leonardo Lucchesi e Jorge Stolfi*

93-23 **Rethinking the DNA Fragment Assembly Problem,** *João Meidanis*

93-24 EGOLib — **Uma Biblioteca Orientada a Objetos Gráficos,** *Eduardo Aguiar Patrocínio, Pedro Jussieu de Rezende*

93-25 **Compreensão de Algoritmos através de Ambientes Dedicados a Animação,** *Rackel Valadares Amorim, Pedro Jussieu de Rezende*

93-26 GeoLab: **An Environment for Development of Algorithms in Computational Geometry,** *Pedro Jussieu de Rezende, Welson R. Jacometti*

93-27 **A Unified Characterization of Chordal, Interval, Indifference and Other Classes of Graphs,** *João Meidanis*

93-28 **Programming Dialogue Control of User Interfaces Using Statecharts,** *Fábio Nogueira de Lucena e Hans Liesenberg*

93-29 EGOLib – **Manual de Referência,** *Eduardo Aguiar Patrocínio e Pedro Jussieu de Rezende*

Relatórios Técnicos – 1994

94-01 **A Statechart Engine to Support Implementations of Complex Behaviour,** *Fábio Nogueira de Lucena, Hans K. E. Liesenberg*

94-02 **Incorporação do Tempo em um SGBD Orientado a Objetos,** *Ângelo Roncalli Alencar Brayner, Claudia Bauzer Medeiros*

94-03 **O Algoritmo KMP através de Autômatos,** *Marcus Vinícius A. Andrade e Cláudio L. Lucchesi*

94-04 **On Edge-Colouring Indifference Graphs,** *Celina M. H. de Figueiredo, João Meidanis, Célia Picinin de Mello*

94-05 **Using Versions in GIS,** *Claudia Bauzer Medeiros and Geneviève Jomier*

94-06 **Times Assíncronos: Uma Nova Técnica para o Flow Shop Problem,** *Hélvio Pereira Peixoto e Pedro Sérgio de Souza*

94-07 **Interfaces Homem-Computador: Uma Primeira Introdução,** *Fábio Nogueira de Lucena e Hans K. E. Liesenberg*

94-08 **Reasoning about another agent through empathy,** *Jacques Wainer*

94-09 **A Prolog morphological analyser for Portuguese,** *Jacques Wainer, Alexandre Farcic*

94-10 **Introdução aos Estadogramas,** *Fábio N. de Lucena, Hans K. E. Liesenberg*

94-11 **Matching Covered Graphs and Subdivisions of K_4 and $\overline{C_6}$,** *Marcelo H. de Carvalho and Cláudio L. Lucchesi*

94-12 **Uma Metodologia de Especificação de Times Assíncronos,** *Hélvio Pereira Peixoto, Pedro Sérgio de Souza*